A high-reflective surface measurement method based on conoscopic holography technology

Xu Cheng, ZhongWei Li, YuSheng Shi, HengShuang Zhao, Guomin Zhan

Xu Cheng, ZhongWei Li, YuSheng Shi, HengShuang Zhao, Guomin Zhan, "A high-reflective surface measurement method based on conoscopic holography technology," Proc. SPIE 9276, Optical Metrology and Inspection for Industrial Applications III, 927608 (13 November 2014); doi: 10.1117/12.2071706

SPIE.

Event: SPIE/COS Photonics Asia, 2014, Beijing, China

A high-reflective surface measurement method based on conoscopic holography technology

Xu Cheng, Zhongwei Li*, Yusheng Shi, Hengshuang Zhao, Guomin Zhan

State Key Laboratory of Material Processing and Die & Mould Technology, Huazhong University of Science and Technology, 430074, Wuhan, China

ABSTRACT

Measuring high-reflective surfaces using optical method is always a big challenging problem. This paper presents a high-reflective surface measurement method based on conoscopic holography technology using a 4D motion platform equipped with a conoscopic holography optical probe. There are two key problems needed to solve before the automate scan of the complex shape surface: the coordinate calibration and the path planning. To improve the calibration efficiency and accuracy, the coordinate calibration is divided into two parts: the rough calibration and the accurate registration. The path planning consists of two aspects including: the path points generation and the path points verification. In addition, by scanning the objects having high-reflective surfaces, such as the metal blades, coins and other work-pieces, the efficiency of the measurement method has been verified.

Keywords: high-reflective surface, conoscopic holography, coordinate calibration, path planning

1. INTRODUCTION

The rapid development of the modern digitizing devices, such as CMM, laser/optical scanning measurement systems, make it possible to measure free-form surfaces qucikly and accurately.[1] While for high-reflective surfaces, the accurate measurement can be a big problem for those devices due to their measuring properties.

There are generally two types of surface measurement methods: contact measurement and non-contact measurement. Contact measurement is a measuring method that acquires surface geometric information by physically touching the parts, such as CMM. Non-contact measurement is used to acquire surface geometric information by using some sensing devices without touching the parts, such as laser/optical scanners.

CMM has high accuracy, repeatability and reliability, it has advantages that it is not affected by the surface properties.[1] While the limitations of CMMs are that they have slower measuring speed than laser or optical scanners. Generally, CMM can acquire 50 $\sim$ 60 points/minute. Compared with the CMM, the laser/optical scanners have much faster measuring speed,[2] while may be affected by the lighting conditions, especially the metal reflection.

According to the above analysis, the key to solve the high-reflective surface measuring problem lies on the faster measuring speed, higher measuring precision and the ability to avoid the metal reflection influence. The above-mentioned shortcomings that accompany CMM or laser/optical scanners can be overcomed by a novel non-contact measuring method called conoscopic holography technology.

In this research, a laser scanner based on conoscopic holography technology was used for high-reflective surface measurement and an automatic scanning system for reverse engineering and inspection of high-reflective surfaces was developed. The system is composed of a laser scanner and a 4-axis motion platform. It can take the automatically coordinate calibration between the design coordinate system (DCS) and the measurement coordinate system (MCS), generate the scanning path and take the scanning process directly, the final measured data is automatically registered to the design model and the manufacture error of the object is eliminated.[3]

The organization of the paper starts with the measurement principle in Section 2. Section 3 illustates the surface measurement method, including the coordinate calibration and the scanning path planning. Section 4 show the parameters of the scanning system and the experiment results. Finally, Section 5 draws conclusions on the research.

Further author information: (Send correspondence to Zhongwei Li)
Zhongwei Li: E-mail: zwli@hust.edu.cn

Optical Metrology and Inspection for Industrial Applications III, edited by Sen Han, Toru Yoshizawa, Song Zhang, Proc. of SPIE Vol. 9276, 927608 · © 2014 SPIE · CCC code: 0277-786X/14/$18 · doi: 10.1117/12.2071706

2. MEASUREMENT PRINCIPLE

2.1 The conoscopic holography technology

The conoscopic holography technology is proposed by G.Sirat and D.Psaltis.[4] Fig. 1 presents the basic principle of a conoscopic hologram setup. Consider a single ray reflected from the point P of an object, the light ray passes through a circular polarizer and generates two orthogonal polarizations, one having a quarter-wavelength relative phase delay. The two rays propagate through a uniaxial crystal, along the same geometrical path, one in the ordinary mode, one in the extraordinary mode, but both with different light velocities owing to the different refractive indices. The ordinary refractive index is constant, whereas the extraordinary refractive index is a function of the direction of the ray relative to the crystal optical axis. These two rays are put into the same polarization mode by a circular analyzer placed after the crustal. Then we record a light pattern result from the interferences between the ordinary and the extraordinary rays. Reconstruction is the process of retrieving the 3D information about the object from the recorded hologram.

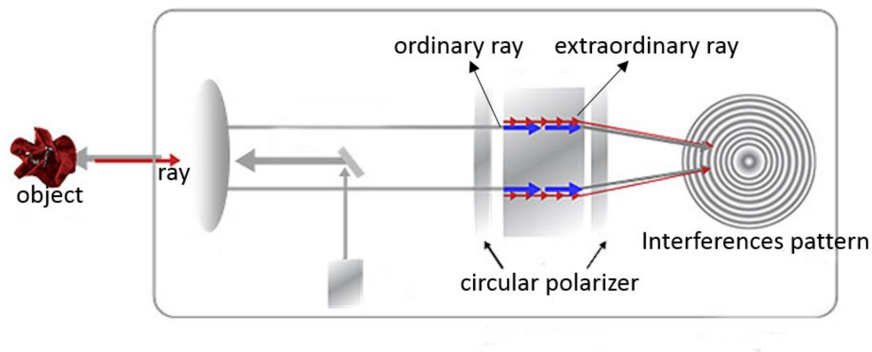

Figure 1. Basic configuration of a conoscopic hologram setup

The conoscopic holography technology has very good properties on measuring surface geometric information. The accuracy of the laser scanners equipped with a 50mm lense can be as good as $6\mu m$, the measuring speed can reach up to 3000 $points/second$ and the measuring angle range on the surface can be as large as $170°$. Most importantly, the measuring results will not be influenced by the surface properties. As it is mentioned above, the accurate measuring result will be directly acquired without spraying powder before, the offset of the powder on the surface is removed.

2.2 System structure

Fig. 2 shows the image of the scanning system. In the 4-axis scanning system, the laser scanner is fixed on the z axis of the motion platform, the rotation axis is parallel to the z axis, the measured object is mounted on the $x-y$ plane. The direction of the laser is paraller to the y axis and perpendiclar to the x axis. The 3 axises are driven by sevro motors, the linear encoders are separately set. In the measuring process, the scanner is moved with the z axis and the measured object is moved with the x, y axises, the distance x_0 between the measured point P and the scanner is acquired and the moving displacement (x, y, z) is detected by the linear encoders so as to take the completely 3D surface measurement ,the position of the measured point P is $(x + x_0, y, z)$. Both of the distance data and the moving displacement data is collected by the communication box and transformed to the computer.

In the coordinate calibration process, the primary procedure is to calibrate the DCS and the MCS. While in practical measurement operation, the measured free-form surface and the design model may have arbitrary 3D locations and orientations,[5] this makes the initial transformation estimation difficult or impractical. In practical applications, localization can be regarded as a two-step process: find the point to point corresponding relationship between measured and designed surfaces[6] and to solve the 3D rigid transformation between these two surfaces to bring them into a common coordinate system. For the above problems, the new method proposed in the paper divided the calibration process into two parts: the rough calibration and the accurate calibration. The

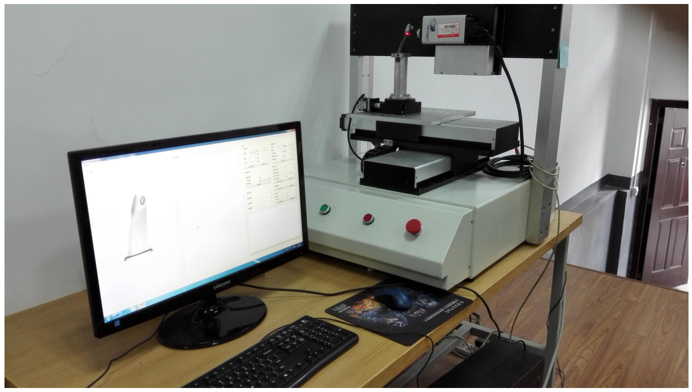

Figure 2. The image of the 3D measuring system

rough calibration manually determines the corresponding points and solves the 3D rigid transformation with the singular value decomposition (SVD) algorithm; in the accurate calibration process, the corresponding point pair between measurement surface and the design model is determined by seaching for the closest point, and the transformation is solved by the minimization of the squared distance between these two surfaces.

In the path planning process, instead of dealing with the entire surface, the surface is approximated by a point cloud sampled in the surface. The goal of the measuring path planning is the generation of the minimum numbers of path points for the complete measurement of the arbitrary specified region, considering of the DOF and the measuring boundary.

3. SURFACE MEASUREMENT METHOD

3.1 The rough calibration

Assumed that the initially measured data of the surface is P, the 3D data of the designed model is Q. The first step for the rough calibration is to manually determine the corresponding points pair, $P_0 = \{p_1, p_2, \ldots, p_n\}$ in the measured data and $Q_0 = \{q_1, q_2, \ldots, q_n\}$. By using the singular value decomposition (SVD) algorithm, the transform relationship between the DCS and the MCS can be represented as,

$$Q_0 = R_0 P_0 + t_0 \tag{1}$$

The R_0 represent the rotation transformation in the rough calibration, the t_0 represent the translation matrix. And the transformation matrix T_0 can be represented with the R_0 and t_0.

$$T_0 = \begin{bmatrix} R_0 & t_0 \\ 0 & 1 \end{bmatrix} \tag{2}$$

3.2 The accurate calibration

After the rough calibration, the measured surface is positioned to fit to the desgin model. With the similar position and orientation, the corresponding relationship is established using the iterative closest point (ICP) algorithm. The ICP algorithm was proposed by Besl and McKay[7] for the registration of 3D shapes. the ICP algorithm updates the correspondence between the objects based on the closest distance at each iteration and iteratively converges to the minimum, it has several termination criteria:[8] 1) The number of iterations has reached the maximum number of iterations; 2) The difference between the previous transformation and the current estimated transformation is smaller than an imposed value; 3) The sum of Euclidean squared errors is smaller than a defined threshold.

According to the above principles, the iterative transformation matrix for each iteration process can be represented as below:

$$T_i = \begin{bmatrix} R_i & t_i \\ 0 & 1 \end{bmatrix}, i = 1, 2, ..., n \tag{3}$$

The transformation relationship between measured surface and the desgin model in the ith iterative process can be fomulated as,

$$Q_i = T_i P_i \tag{4}$$

Assuming that after Nth iteration the algorithm come to the termination, then the correspondence between the initial positon and the final position of the object is:

$$Q_N = \prod_{i=1}^{N} T_i P_1 \tag{5}$$

P_0 is the inital position of the measured surface, P_1 is the postion of the measured surface in the $1th$ iterative process, the corresponding relationship between P_0 and P_1 is just the rough transformation,

$$P_1 = T_0 P_0 \tag{6}$$

So the accurate transformation between the measured surface and the designed model is,

$$Q = \prod_{i=1}^{N} T_i P \tag{7}$$

Fig. 2 shows the whole coordinate calibration process.

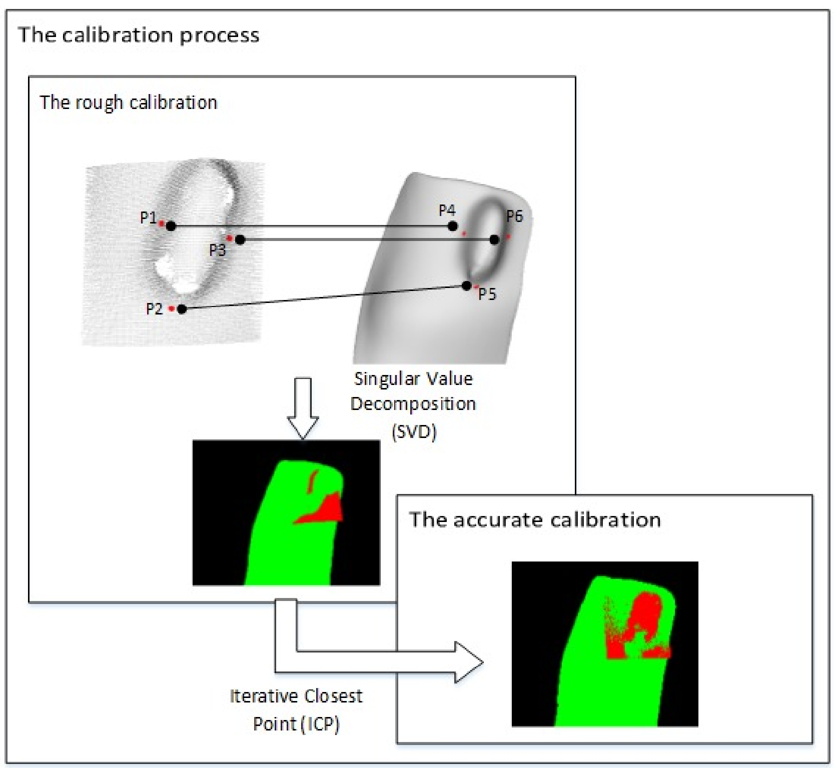

Figure 3. The whole coordinate calibration process

3.3 The path planning

As it is formulated above, the surface is approximated by a point cloud sampled in the surface. The scanning path is the collection of line segments that guide the laser probe during the measuring process.[9] For the laser probe can only capture the 3D position of one point each time, it is impractical for the system to measuring the

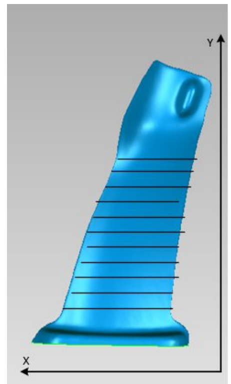

Figure 4. Curve segments division

whole surface uniformly. So the scanning path will be generated by dividing the free-form surface into a series of curve segments with a constant distance along the $\vec{z}$ direction as the Fig. 3 shows. For each line segment, the points are uniformly sampled along the $\vec{x}$ direction, then whether the sampled points are in the DOF or not is detected.[10]

The main steps of the scanning path generation are as below:

Step 1 Choose the bottom and top line along the $\vec{z}$ direction as the scanning boundary;

Step 2 Set the gap between the two neighbor line segments;

Step 3 For the $i\ th$ line segment, assign the first point as the begining point;

Step 4 Assign the next point as the end point;

Step 5 Detect whether the present point is in the DOF, is yes return to Step 3; if no,adjust the point position to the center of the DOF, assign i to be $i+1$ and return to Step 2.

Step 6 Export the generated path after the end of the iteration process.

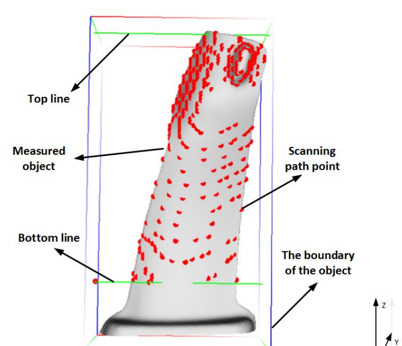

Figure 5. example of the generated scanning path

The Fig. 5 shows an example of the generated scanning path. The colorful cuboid shows the geometric boundary of the measured object, the two green lines are seperately the top and the bottom line of the scanning boundary and the red points on the surface are the key points which are the projection results of the scanning path points. In the scanning process, the scanners take the measurement backwards and forwards along the $\vec{x}$ direction and gradually increase its height along the $\vec{z}$ direction, the $i+1\ th$ line segment is scanned after the $i\ th$ line segment is finished.

4. EXPERIMENT

The proposed algorithm are demostrated by applying them to the examples. The gap between the neighbor line segment along the $\vec{z}$ is set to be $0.5mm$. The scanner used for experiment is ConoProbe Mark3.0 manufactured by OPTIMET, Inc. It has a view angle limit of $170°$, accuracy of $6\mu m$, standoff distance of $42mm$, depth of field of $8mm$, maximum data acquiring speed of 3000 $points/second$. The motion displacement of the platform is $300 * 300 * 300\ mm$, the motion platform's positional accuracy is $0.01mm$.

4.1 Application example

In the application example, an aerospace blade with its design model prior known is measured. Fig. 6 seperately shows the image of the measured object, the measurement result and the 3D mesh model of the blade.

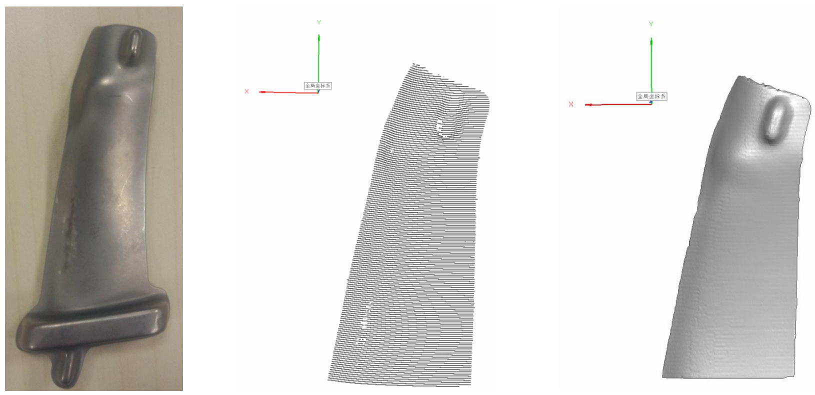

(a) image of the object (b) measured result (c) 3D mesh model

Figure 6. Measurement results

Additionally, to examine the ability of the measuring system for high-reflective surface measurement, a metal coin and a metal craft is measured. Fig. 7 shows the measurement results of the two objects, Fig. 7(a) shows the measured metal coin and Fig. 7(b) shows the measured metal craft.

(a) image of the object (b) measured result

Figure 7. Measurement results

4.2 Error analysis

By automatically register the acquired data, the difference between the object and the design model is analysised and shown in Fig. 8. The root mean square (RMS) value of the error is 0.030 mm. It's obvious that the accuracy of the measurement system for high-reflective surface has been verified.

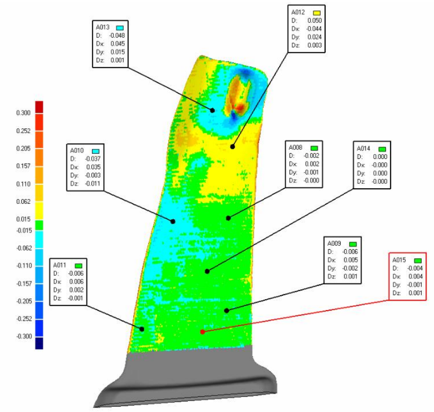

Figure 8. Error analysis

5. CONCLUSION

In this paper, an automatic 3D scanning system for reverse engineering and inspection of high-reflective surfaces has been developed. The two-steps coordinate calibration method was used for the accurate localization of the DCS and MCS. The design model was transformed to the MCS to direct the measurement process. A path planning algorithm was proposed to generate the scanning path that ensured the whole scanned surface region was in the DOF. The experiment results approve that the system can achieve the automatic measurement of the high-reflective surfaces. The measurement error is within 0.03mm.

ACKNOWLEDGMENTS

This work was supported by the Program for Changjiang Scholars and Innovative Research Team in University (Grant No.IRT1244), the Fundamental Research Funds for the Central Universities, HUST (Grant No.CXY13Q039), National Science and Technology Major Project of China (Grant No.2013ZX02104004003_IC) and the Major program of Science and Technology Planning Project of Hubei province (Grant No.2013AEA003).

REFERENCES

[1] Y. Li and P. Gu, "Free-form surface inspection techniques state of the art review," *Computer-Aided Design* **36**(13), pp. 1395–1417, 2004.

[2] Z. Li, Y. Shi, C. Wang, D. Qin, and H. Kui, "Complex object 3d measurement based on phase-shifting and a neural network," *Optics Communications* **282**(14), pp. 2699–2706, 2009.

[3] Y. Li and P. Gu, "Automatic localization and comparison for free-form surface inspection," *Journal of manufacturing systems* **25**(4), pp. 251–268, 2006.

[4] G. SIRAT, "Conoscopic holography. i: Basic principles and physical basis," *Journal of the Optical Society of America* **9**(1), pp. 70–83, 1992.

[5] K. H. Ko, T. Maekawa, and N. M. Patrikalakis, "An algorithm for optimal free-form object matching," *Computer-Aided Design* **35**(10), pp. 913–923, 2003.

[6] Myronenko, Andriy, and X. Song, "Point set registration: Coherent point drift," *IEEE Transactions on Pattern Analysis and Machine Intelligence* **324**(12), pp. 2262–2275, 2010.

[7] P. J. Besl and N. D. McKay, "Method for registration of 3-d shapes," *IEEE Transactions on Pattern Analysis and Machine Intelligence* **14**(2), pp. 239–256, 1992.

[8] A. Aldoma and et al, "Tutorial: Point cloud library: Three-dimensional object recognition and 6 dof pose estimation," *Robotics and Automation Magazine* **19**(3), p. 80, 2012.

[9] S. Son, H. Park, and K. H. Lee, "Automated laser scanning system for reverse engineering and inspection," *International Journal of Machine Tools and Manufacture* **42**(8), pp. 889–897, 2002.

[10] K. H. Lee and H. pung Park, "Automated inspection planning of free-form shape parts by laser scanning," *Robotics and Computer-Integrated Manufacturing* **16**(4), pp. 201–210, 2000.